Pergamon

Cement and Concrete Research 29 (1999) 1077–1083

CEMENT AND CONCRETE RESEARCH

Fatigue behavior of polymer-modified porous concretes

Miguel Ángel Pindado, Antonio Aguado, Alejandro Josa*

Universitat Politècnica de Catalunya (UPC), School of Civil Engineering (ETSECCPB), Jordi Girona 1-3, Módulo C1, E-08034 Barcelona, Spain

Received 28 January 1997; accepted 5 April 1999

Abstract

Highly permeable materials provide drainage and noise-absorption properties that are useful in pavement top layers. In such porous concretes, the voids reduce the mechanical integrity, which may have to be compensated for with the incorporation of nonconventional components, such as polymers. A basic property needed for the design of pavements is the fatigue behavior of the material, which has not been studied thoroughly for polymer-modified porous concretes. This paper presents experimental results of fatigue tests in compression in terms of Wöhler curves for four porous concretes (two of them with polymer). It is seen that the polymer-modified porous concretes exhibit better fatigue behavior than those without polymer. However, the improvement decreases for low values of the stress level, S, and appears to be negligible for the case of traffic loads in main roads or highways (number of load cycles, $N > 10^6$). Additionally, the deformation and internal temperature evolutions have been monitored, and it is concluded that their trends are similar to those of conventional concrete, with temperature increases significantly higher than in conventional concretes.

Keywords: Fatigue; Porous concretes; Polymers; Silica fume; Thermal analysis

"Porous concretes" are materials with the same basic components as conventional concretes but designed to have high porosity and permeability. The porosity is achieved by using a gap-graded aggregate distribution in which there is a very low proportion of fine aggregates. In practice, this type of concrete has been used in shoulders, bases, and subbases of roads and highways, taking advantage of its drainage properties [1–5]. A more recent application in which both drainage and noise absorption are relevant is as the top layer or overlay of concrete pavements [6–10], similar to that of porous asphalt.

Along with the high porosity and permeability, appropriate mechanical strengths and durability must be guaranteed in the concretes [9,11,12]. However, when the porosity increases, the mechanical strength tends to decrease. For this reason, porous concretes may require a new component, for instance a polymer or microsilica. The use of polymers is a good solution but the high associated costs restrict their use to thin top layers bonded to a bottom layer of conventional concrete [6,13].

As considered in different design codes [14,15], an important requisite due to the effect of traffic on pavements is the fatigue behavior. The fatigue of conventional concrete has been studied extensively in the literature. However, few references are available about the fatigue behavior of porous concretes [16], and the trends of conventional concrete cannot be readily extrapolated to them. For example, in conventional concrete, the fatigue life decreases with an increase in air or void content [17], which is not necessarily true in porous concrete [13,18]; its mechanical behavior depends on the aggregate skeleton, and the intergranular contact is strengthened by the mortar, while in conventional concrete the air content generally weakens the material.

The aim of this paper is to evaluate the effects of the incorporation of a polymer on the fatigue behavior of porous concretes and to determine the Wöhler fatigue curves to be used in pavement design. The compressive test is chosen as the basis for this study since it yields the least amount of scatter in the results when compared to other tests such as flexure [19]. Moreover, fatigue life is more or less the same in compression and tension (including splitting and flexure) when expressed as a fraction of the corresponding static strength [20]. These aspects are important since the scatter in fatigue results (Wöhler curves) is mainly attributed to the scatter in the static strength [20]. The study is part of an extensive project on the optimization of mix design and characterization of mechanical, durability, and noise absorption properties of polymer-modified porous concretes. Other re-

* Corresponding author. Tel.: +34-93-401-7260; fax: +34-93-401-7251.
E-mail address: josa@gauguin.upc.es (A. Josa)

0008-8846/99/$ – see front matter
PII: S0008-8846(99)00095-2

sults from the project have been presented elsewhere [13,21,22].

1. Methods

1.1. Materials

The details of the components and the mix proportions used have been reported elsewhere [21,22] and are summarized in Table 1. Since institutions from Germany, The Netherlands, and Spain participated in the project, commercially available components from these countries were used in this study. Mixes 1 and 2 were made with Spanish materials and mixes 3 and 4 were made with Dutch and German materials, respectively. Mix 1, used as the reference, did not contain any polymer. Mixes 2 and 3 had 13.3 and 23.4 kg/m^3 of polymer, respectively. Mix 4 contained microsilica. The polymer used was an acrylic copolymer dispersed in water (FORTON VF-774) and manufactured by DSM Resins (Barcelona, Spain), with the characteristics summarized in Table 2. This polymer was selected on the basis of previous experimental work [13,21,22]. Note that the use of another polymer or type of polymer would presumably have led to different results.

In mix 1, a melamine-based superplasticizer (SIKA 300, Sika, Madrid, Spain), which meets ASTM C 494 requirements for Type F admixture, was used in order to obtain a workability similar to that of mix 2. The density and cylinder compressive strength of each concrete at the age of 28 days are given in Table 1. All mixes were intended to have the same porosity (about 25%) to be able to isolate the influences of the polymer and microsilica used.

1.2. Specimen preparation

The specimens of mix 3 were cast in the Intron laboratory in Sittard, The Netherlands and those of mix 4 in the VDZ laboratory in Düsseldorf, Germany. They were shipped for testing to the Structural Technology Laboratory (Barcelona, Spain), where the specimens of the other mixes were fabricated. All concretes were prepared in vertical axis mixers with total mixing times of 1.5 min. The specimens were cylinders cast in 150 × 300-mm molds. Mixes 1, 2, and 4 were compacted with a vibrating hammer in two layers and mix 3 was compacted on a vibrating table. The consistency of the fresh concrete was determined through the Walz test (ISO Test Standard 4111). After compaction, all the specimens were maintained for 1 day in the molds at 20°C. Later the specimens were demolded; mix 2 were cured at 50% relative humidity, mix 3 at 65% relative humidity, and mix 4 was cured under water for 6 days and subsequently at 65% relative humidity. In all cases, the ambient temperature during curing was 20°C. The curing of the specimens of mixes 3 and 4 was interrupted for transportation at the age of 28 days, after which they were maintained at 50% relative humidity along with those of mix 2 until testing. Specimens of the reference concrete, mix 1, were maintained in a fog room (at 98% relative humidity) after demolding until testing. The age at testing varied from 1 to 3 months. Before the test, the flat faces of the cylinder were capped with a sulfur compound.

Table 2
Polymer characteristics

Concentration (by mass)	51% solids, 49% water
Appearance	Milky white
Odour	Mild
Viscosity at 25°C	150 mPa · s
Acidity (acid value or pH)	4.5–5.5
Minimum film = forming temperature	7°C
Size polymer particles	150–200 nm
Density (solids) at 20°C	1136 kg/m^3
Working temperature range	5 < T < 40°C

1.3. Testing procedure

All tests were performed in an INSTRON 8505 Digital Servohydraulic Testing System with a dynamic capacity of 1 MN. The ratio between the minimum and the maximum stress levels (R) was chosen to be small, equal to 0.05, in the fatigue tests in order to simulate the nature of the loading-

Table 1
Mix proportions used and properties

	Mix proportions/properties			
Component/property	1	2	3	4
Gravel type and content (kg/m^3)	Crushed granite (5–12 mm), 1427	Crushed granite (5–12 mm), 1506	River gravel (4–8 mm), 1352	Crushed basalt (5–8 mm), 1534
Sand type and content (kg/m^3)	Crushed limestone (0–5 mm), 101	Crushed limestone (0–5 mm), 106	River sand (0–1 mm), 89	River sand (0–2 mm), 77
Cement type and content (kg/m^3)	Spanish V-35 (40% fly ash), 350	Spanish V-35 (40% fly ash), 275	CEM II 32.5 R, 279	German PZ 35 F (CEM I 42.5), 280
Water (l/m^3)	110	78.5	64	95
Polymer (kg/m^3)	–	13.3	23.4	–
Superplasticizer (l/m^3)	3.5	–	–	–
Microsilica (kg/m^3)	–	–	–	28
Density (kg/m^3)	1980	1930	1815	2070
Compressive strength (28 day, MPa)	26.8	20.6	23.2	13.9

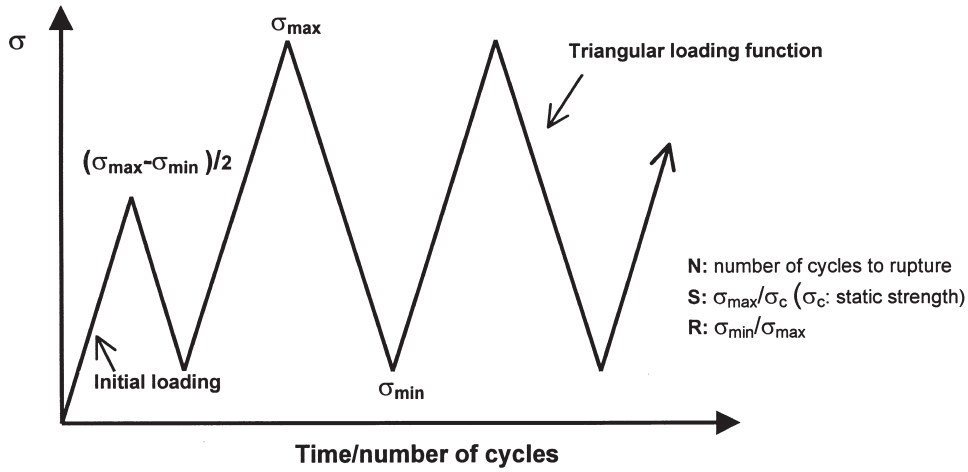

Fig. 1. Loading history and fatigue variables.

unloading cycles due to traffic. However, some tests with mix 2 were conducted with $R = 0.2$ and 0.5 to study the effect of the stress ratio. Maximum stress levels ranging from 60 to 95% of the static strength were used. The fatigue tests were carried out in dry conditions and no special measures were adopted to prevent moisture loss. Since loading frequencies in the range of 1 to 15 Hz have little effect on the fatigue life of concretes [20], a frequency of 15 Hz was selected for the tests in order to reduce their duration. However, a frequency of 10 Hz had to be used for the stress ratio $R = 0.05$ because of limitations of the testing machine. The loading function was triangular as shown in Fig. 1, along with the definitions of the fatigue variables. A maximum of 2 million cycles was imposed for limiting the test durations.

The specimens were grouped according to their composition and age at testing, and for each group the corresponding static strength (σ_c) was determined through standard monotonic tests (according to ISO Standards) of a minimum of three specimens. This strength was used as the reference for the applied stress level ($S = \sigma_{max}/\sigma_c$, where σ_{max} is the maximum stress applied in each cycle) of the fatigue test. The maximum coefficient of variation in these static tests was 3%.

The deformation of the specimen was measured from the piston displacement and corresponded to the total deformation, including the capping layers. The maximum and minimum values in each cycle were registered during the test. In some specimens, the temperature was also monitored by introducing thermocouples to a depth of about 2 cm from the surface. Three thermocouples were placed in each specimen, along a vertical line, near the top and bottom faces and in the center. The ambient temperature was also registered.

2. Results and discussion

2.1. Fatigue life

The observed fatigue behavior was characterized through Wöhler, or *S-N*, curves, which plot the number of cycles to failure (log*N*) for each applied stress level S ($=\sigma_{max}/\sigma_c$). Each Wöhler curve was defined with the log*N* values for five or six S values ranging from $S = 0.6$ to $S = 0.95$; for every S value, one to five tests were performed. The analytical expressions for the curves (in the form $S = a \log N + b$) were obtained through linear regression, using the values of S and log*N* of the tests. The parameters of the fits are given in Table 3. Additionally, the confidence interval of each curve was obtained using statistical analysis.

Fig. 2 shows the *S-N* curves for mix 2 at $R = 0.5$, 0.2, and 0.05. To make the figure clearer, individual results have not been included. It can be seen that the fatigue life increases when R increases; that is, for a constant value of σ_{max}, the fatigue life increases with a decrease in the amplitude of the loading cycle. Moreover, it can be seen that for small values of N, the *S-N* curves tend to converge to S values that are greater than 1. This is mainly because the compressive strength used as a reference was obtained from

Table 3
Parameters of the *S-N* curves ($S = a \log N + b$; R, correlation coefficient)

	Mix 1			Mix 2			Mix 3			Mix 4		
R	*a*	*b*	*R*	*a*	*b*	*R*	*a*	*b*	*R*	*a*	*b*	*R*
0.05	−0.050	0.920	0.806	−0.069	1.080	0.841	−0.057	1.003	0.834	−0.054	0.935	0.950
0.2				−0.065	1.084	0.958						
0.5				−0.050	1.058	0.947						

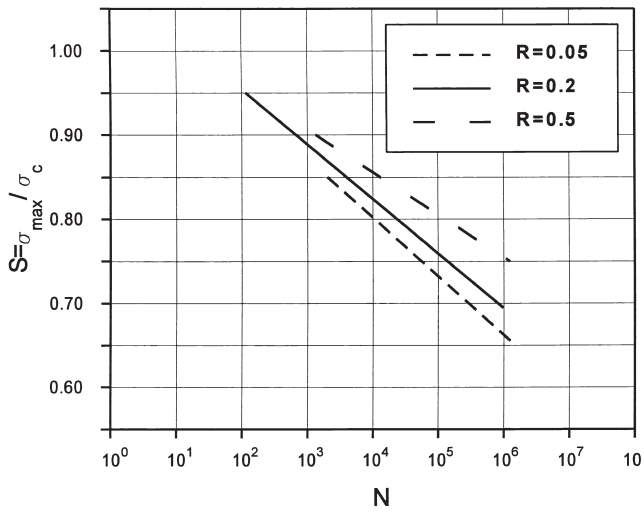

Fig. 2. *S-N* curves of mix 2, at $R = 0.05$, 0.2, and 0.5.

static tests in which the loading rate is much lower than that of the fatigue tests.

Fig. 3 shows the experimental data points, the corresponding *S-N* curves, and the 90% confidence interval obtained for each mix at $R = 0.05$. The data corresponding to specimens that did not reach failure after approximately 2×10^6 cycles are represented with a point and an arrow; these points have been considered in the linear regression analysis of the *S-N* curves as plotted.

Fig. 4 shows all the *S-N* curves of Fig. 3 in the same plot. It can be observed that the addition of polymers improves the fatigue behavior of porous concrete. In other words, for a certain value of *S* the fatigue life (*N*) of the porous concrete with polymer (i.e., mixes 2 and 3) is improved in comparison with the concrete without polymer (mixes 1 and 4). The improvement is not constant in the entire range of *S* values tested but is maximum (by approximately one order of magnitude) at high values of *S* and decreases with a decrease in *S*. This trend has also been observed in polymer concretes under flexure [23]. Also, the difference between the behaviors of the two polymer-modified concretes mixes 2 and 3 is small.

Since the concretes had practically the same porosity and the aggregate gradings were not very different, the variations in the static strength and, in general, the mechanical behavior can be attributed to the differences in the composition of the matrices. The changes in the ductility and/or creep behavior of the matrix produced by the incorporation of the polymer [24] probably lead to the observed improvement in the fatigue behavior of the concrete. An increase in the ductility can be expected to decrease the rate of evolu-

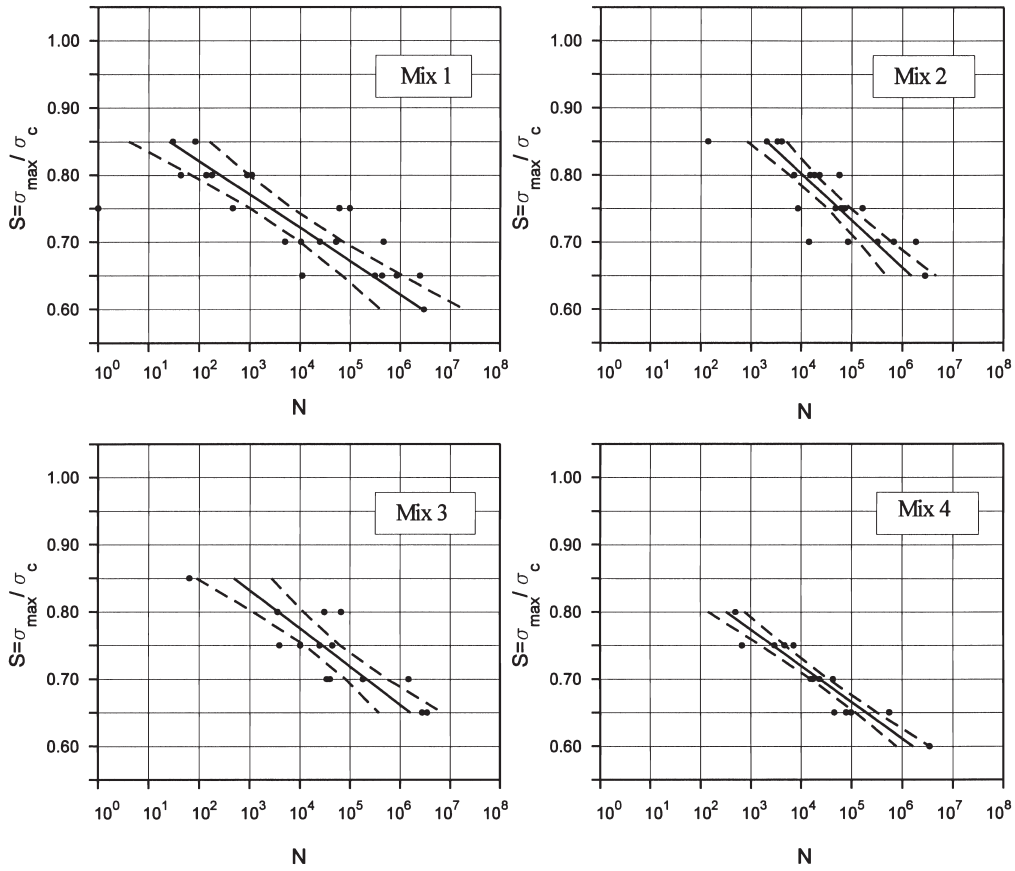

Fig. 3. *S-N* curves and 90% confidence intervals at $R = 0.05$. The black points represent the one to five tests that were performed.

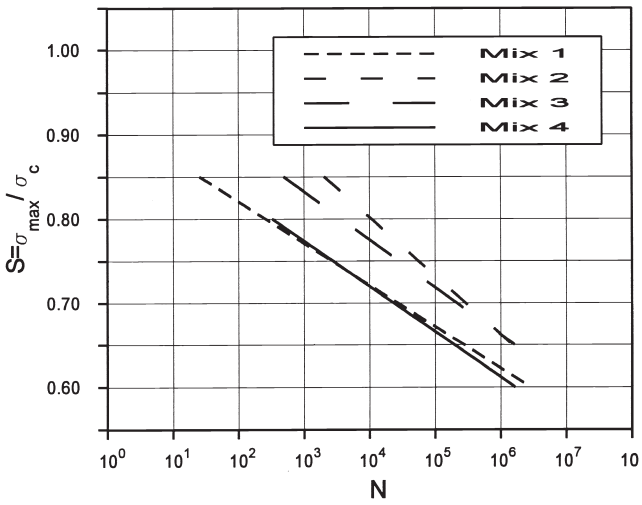

Fig. 4. *S-N* curves for $R = 0.05$.

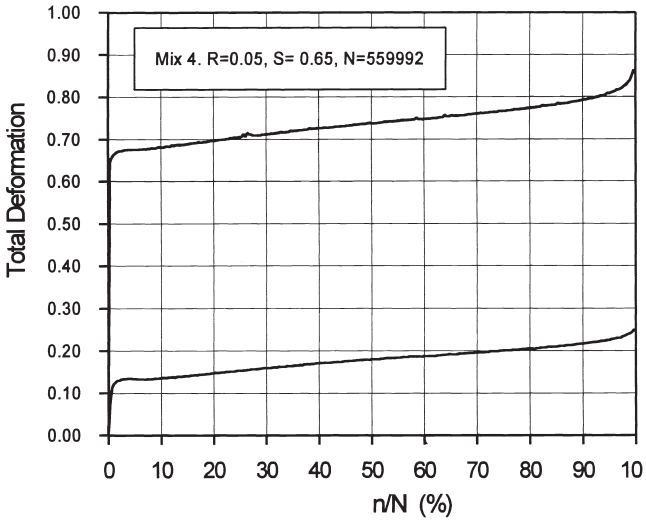

Fig. 5. Maximum and minimum total deformation evolution during a test.

tion of damage, especially at higher values of S (i.e., higher loading rates), leading to higher values of N. On the other hand, at low values of S (i.e., low loading rates), which correspond to the case of traffic loads in main roads or highways, an increase in the creep deformation due to the polymer would lead to lower or negligible improvements.

The behavior of the two mixes without polymer (1 and 4) is practically identical, suggesting that the incorporation of microsilica (in mix 4) does not significantly modify the fatigue behavior of concretes studied here.

2.2. Evolution of deformations

Fig. 5 shows the typical evolution of the maximum and minimum deformations in each cycle as a function of the number of cycles for a specimen of mix 4 corresponding to $S = 0.65$ and $N = 559{,}992$ cycles. The trend confirms the presence of three distinct stages in the evolution of deformations during the cyclic loading, as seen in conventional concrete [25]. In the first stage, the deformations increase rapidly until about 5% of the fatigue life, then stabilize until about 95% of the life. After that the deformations again increase rapidly up to failure.

2.3. Thermal behavior

It was observed that during cyclic loading the specimens exhibited a significant increase in temperature, indicating that part of the energy consumed was dissipated as heat, as in conventional concrete [26]. However, no reports have been found in the literature of temperature increases as high as in those observed in this study. In order to quantify the temperature evolutions, thermocouples were placed in some of the specimens as explained earlier. The maximum temperatures registered in the concretes were as high as 50°C in the tests of specimens from mixes 1 and 2 (at ambient temperatures of about 23°C). Fig. 6 shows the temperatures registered by the three thermocouples in a specimen of mix 3 ($R = 0.05$) subjected to $S = 0.70$, which failed after 1,493,113 cycles. The maximum temperatures occur at the middle of the specimen, where there is the least confinement due to the friction between the loading plattens and the specimen. Also, the temperature is slightly higher at the upper thermocouple than at the lower one, which can be attributed to the fact that the upper loading platten could rotate while the lower platten was fixed, leading to more deformations in the upper part of the specimen. This is supported by the fact that more damage was observed in the upper halves of the specimens. Comparing the temperature evolutions with those of the deformations (Fig. 5), it can be seen that the trends are similar with three distinct stages.

At higher values of S, where the fatigue life is much shorter, the temperature increases monotonically throughout the duration of the test, without exhibiting the stabilized

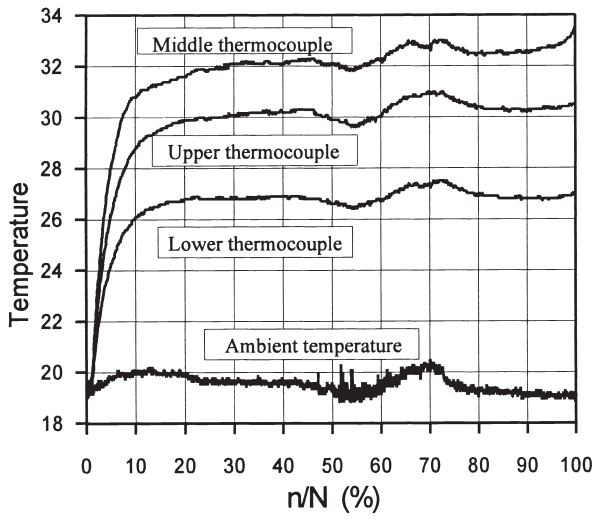

Fig. 6. Evolution of temperature in a specimen of mix 3.

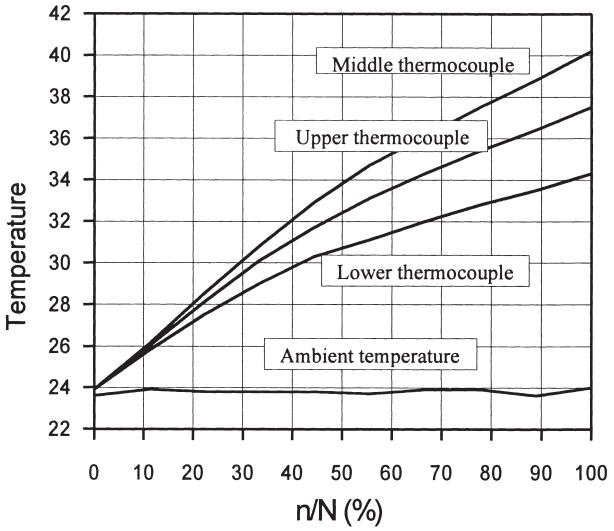

Fig. 7. Evolution of temperature in a specimen of mix 2.

stage seen in Fig. 6. For example, in Fig. 7 corresponding to a specimen of mix 2 with $R = 0.05$ and $S = 0.80$, which failed after 56,465 cycles, all three thermocouples reflect a continuous increase in temperature. In other specimens, maximum temperature differences of 15 to 30°C, between the center of the specimen and the environment were observed.

The increase in the specimen temperature can be expected to depend on the frequency and rate of loading. Nevertheless, the measured temperature evolutions also reflect the effect of the amount of heat that can be transferred to the environment during each loading cycle. This would be lesser for higher frequencies and faster loading rates, leading to higher temperature distributions in these cases. Accordingly, it would be better to perform the fatigue tests at lower frequencies (which simulate the traffic loading better) to avoid undesired effects of the higher temperatures on the mechanical behavior.

3. Conclusions

- The fatigue behavior of porous concrete is adequately represented by Wöhler curves in terms of linear relations between the maximum stress level S and log$N$, where N is the fatigue life in cycles. The slope of the curves depends on the stress ratio of the cyclic loading as in the case of conventional concretes.
- For larger values of S, polymer modified porous concretes exhibit better fatigue behavior than those without polymer. However, the improvement decreases for lower values of S and appears to be negligible for the case of traffic loads in main roads or highways ($N > 10^6$). This behavior is probably due to changes in the ductility and creep behavior of the matrix induced by the incorporation of the polymer.
- The two porous concretes studied here without any polymer, one with microsilica and the other without, exhibited similar fatigue behavior.
- In tests with low values of S, the evolution of the axial deformations and the internal temperature of the concrete specimens exhibit three distinct stages, with rapidly increasing first and third stages and a metastable second stage. In tests with high S values, the second stage tends to vanish.
- The internal temperature of the concrete increased with the number of cycles. This increase was significantly higher than in conventional concretes. Moreover, the temperature distribution was not constant over the height of the specimen and the maximum temperatures occurred in the middle. Also, higher temperatures were observed in the upper half of the specimen due to the lack of symmetry of the loading produced by a moving upper platten and a fixed lower platten. In order to avoid undesired effects due to the increase of temperature, it seems advisable to use lower frequencies for simulating the traffic loading.

Acknowledgments

The financial assistance for the present work was provided by the Brite-Euram BE-3415 project of the European Commission, the Spanish CICYT grant MAT93-0293, and a project of the Instituto Español del Cemento y sus Aplicaciones (IECA). An FPI grant from the Ministerio de Educación y Ciencia (Spain) to the first author is also appreciated. The authors would like to thank Mr E. Eickschen (VDZ, Germany) and Mr E. Onstenk (Intron, The Netherlands), who participated in the experimental part of the Brite-Euram project. The authors are grateful to Dr. W.L. Repette and Dr. R. Gettu for their detailed and very useful reviews of previous versions of this paper.

References

[1] A. Jasienski, L'usage du béton poreux en bandes d'arrêt d'urgence (B.A.U.), Technique Routiére 1 (1984) 6–15.
[2] W.H. Ames, Concrete pavement design and rehabilitation in California, 3d Int. Conf. on Concrete Pavement Design and Rehabilitation, Purdue Univ., West Lafayette, 1985, pp. 253–265.
[3] G. Raimbault, J.L. Nissoux, B. Barbe, Les chaussées poreuses. Une technique nouvelle pour l'assainissement urbain, Bull Liaison Laboratoires de Ponts et Chaussés 117 (1982) 21–31.
[4] M.D. Mathis, Permeable base design and construction, 4th Int. Conf. on Concrete Pavement Design and Rehabilitation, Purdue Univ., West Lafayette, 1989, pp. 663–670.
[5] L. Hendrikx, Use of porous concrete road bases in Belgium, 8th Int. Symp. on Concrete Roads (Lisbon), Cembureau, Brussels, Theme II, 1998, pp. 65–67.
[6] G.H. Kellersman, F. Smits, An experiment with porous concrete toplayer on J.C.P., 4th Int. Conf. on Concrete Pavement Design and Rehabilitation, Purdue Univ., West Lafayette, 1989, pp. 615–624.
[7] G. Pipien, J.P. Christory, F. Combelles, G. Raimbault, Routes à structures poreuses. Où en est-on? Revue Générale des Routes et des Aerodromes 694 (1992) 1–8.

[8] E. de Winne, Cement concrete hardenings with reduced noise pollution in the Flemish community, in: R.K. Dhir, N.A. Henderson (Eds.), Concrete for Infrastructure and Utilities, E & FN Spon, London, 1996, pp. 141–150.
[9] L.A. Solís, A. Llorente, J. Días Minguela, M. Bollati, High performance porous concrete for heavy traffic, ring road of Segovia, 8th Int. Symp. on Concrete Roads (Lisbon), Cembureau, Brussels, Theme V, 1998, pp. 203–217.
[10] S. Riffel, Draining concrete—the material for today's and tomorrow's roads, quiet—safe—environment-friendly—production—characteristics—applications, 8th Int. Symp. on Concrete Roads (Lisbon), Cembureau, Brussels, Theme V, 1998, pp. 103–110.
[11] G. Raimbault, J.D. Balades, A. Faure-Soulem, Quatre expérimentations françaises de chaussées poreuses, Bull Liaison Laboratoires de Ponts et Chaussés 137 (1995) 43–55.
[12] M.R. Bollati, R. Talero, M. Rodriguez, B. Witoszek, F. Hernandez, Porous high performance concrete for road traffic, in: R.K. Dhir, N.A. Henderson (Eds.), Concrete for Infrastructure and Utilities, E & FN Spon, London, 1996, pp. 589–599.
[13] Brite-Euram Project BE 3415, Surface properties of concrete roads in accordance with traffic safety and reduction of noise, State-of-the-Art Report, Recommendations for Practice and Further Developments and Final Technical Report, Intron, Sittard, The Netherlands, 1994.
[14] Portland Cement Association, Thickness Design for Concrete Highway and Street Pavements, Portland Cement Association, Skokie, 1984.
[15] American Association of State Highway and Transportation Officials, Guide for Design of Pavement Structures, American Association of State Highway and Transportation Officials, Washington, 1986.
[16] J.L. Nissoux, P. Merrien, Les bandes d'arrêt d'urgence en béton poreux. Étude du matériau, Bull Liaison Laboratoires de Ponts et Chaussés 92 (1977) 142–148.
[17] F.W. Klaiber, D.Y. Lee, The Effects of Air Content, Water-Cement Ratio and Aggregate Type on the Flexural Fatigue Strength of Plain Concrete, ACI SP-75, American Concrete Institute, Farmington Hills, 1982, pp. 111–131.
[18] J.J. Rosell, A. Aguado, J. Dolz, Características mecánicas del hormigón poroso, Ingeniería Civil 63 (1987) 82–88.
[19] R.C. Meininger, N.R. Nelson, Concrete mixture evaluation and acceptance for air field pavements, in: Aircraft/Pavement Interaction: An Integrated System, Proc. ASCE Conference (Kansas City), American Society of Civil Engineers, New York, 1991, pp. 199–224.
[20] Comité Euro-International du Béton, Fatigue of concrete structures, State of the Art Report, Bulletin d'Information No 188, Comité Euro-International du Betón (CEB), Lausanne, 1988.
[21] E. Onstenk, A. Aguado, E. Eickschen, A. Josa, Laboratory study of porous concrete for its use as top-layer of concrete pavements, 5th Int. Conf. on Concrete Pavement Design and Rehabilitation, Vol. 2, Purdue Univ., West Lafayette, 1993, pp. 125–139.
[22] A. Josa, E. Onstenk, C. Jofré, E. Eickschen, A. Aguado, Porous top-layer for concrete pavements—laboratory study and structural analysis, Int. Conf. Concrete Across Borders (Odense), Vol. 1, Danish Concrete Association, Copenhagen, 1994, pp. 205–214.
[23] H.T. Hsu, Flexural behaviour of polymer concrete beams, Ph.D. Thesis, The University of Texas at Austin, 1983.
[24] American Concrete Institute, Polymers in Concrete, American Concrete Institute, Farmington Hills, 1977.
[25] J.K. Kim, Y.Y. Kim, Experimental study of the fatigue behavior of high strength concrete, Cem Concr Res 26 (10) (1996) 1513–1523.
[26] R. Tepfers, B. Hedberg, G. Szczekocki, Absorption of energy in fatigue loading of plain concrete, Materials and Structures 17 (97) (1984) 59–64.